

TOPOLOGICAL GRADIENT OPERATORS FOR EDGE DETECTION

Hakan Guray Senel

Department of Electrical Engineering
Anadolu University
Eskisehir, Turkey

ABSTRACT

Edge detection in image processing is the task of locating pixel value variations in images. First methods were directional derivative based linear filters. One of the most important problems of these methods that are based on computation of approximate derivative are their sensitivity to noise due to small kernel sizes. Small kernels are widely used to avoid the effect of nearby objects. In this work, we propose a fuzzy topology based method that allows the use of larger gradient kernels. This method produces thin gradient lines by limiting the support area of gradient kernels for slowly varying ramp-like edges. By applying the proposed method on synthetic and natural images, it is observed that it decreases the output area around the edge and has a better noise suppression compared to conventional gradient operators.

Index Terms— Edge detection, fuzzy image topology

1. INTRODUCTION

Edge detection is the process of localizing pixel intensity transitions. The success of edge detection provides a good basis for the performance of higher level image processing tasks such as object recognition, target tracking and segmentation, since it reduces the amount of information to be processed. Over the years, many methods have been proposed for edge detection [1,2].

Typically, edge detection is performed by computing an edge image by a linear filter that is an approximation of a first or a second order derivative. Then a decision stage, which requires an application of a threshold, takes place. Due to the sensitivity of derivative operators to noise, a smoothing step may also be needed prior to derivative calculation. While the smoothing operation suppresses noise and removes small details, it may cause localization errors.

Most conventional edge detectors are based on some edge and noise model. The most common model is an ideal step edge contaminated with Gaussian noise as in the case

of Canny filter [1]. Some edge detection methods also assume that only one edge structure is contained within the boundaries of an operator kernel. In order to satisfy this assumption, kernel sizes are selected as small as possible. This model is very restrictive for two reasons. Firstly, in most images there are smoothly varying edges. Secondly, the presence of neighboring objects in the scene contradicts with the model of having a single step function within an observation window. The influence of neighboring objects in the scene may introduce a considerable impact on the edge detection process [3].

If a gradient kernel with a small support is applied on an image that is corrupted by noise, disconnected and spurious edge information may be obtained. This is mainly due to the fact that limited number of pixels is used in the process and noisy pixel values may dominate in the gradient calculation. Small operators, such as 2x2 Roberts, 3x3 Sobel and Prewitt are often used, even though they are known to be adversely affected by noise [4]. Using larger masks are often discouraged since they can increase the possibility of interference from neighboring edges [5].

Although narrow operators are best for describing detailed texture, wide operators report low-amplitude responses more reliably [6]. By using kernels with larger supports (e.g. 11 x 11 or 13 x 13), it is possible to design edge detection schemes that yield good performance in three respects: accuracy in derivative calculation, handling of slowly varying edges and good noise immunity. Immunity to noise is also needed for tolerating deviations from edge models [7]. If narrow operators are employed in the edge detection process, ideal step edges are only taken into consideration. If the edge is not fully contained in the mask due to sampling reasons, the response of the operator may be adversely affected.

2. FUZZY TOPOLOGY AND DOCM

The notion of connectedness is a fundamental concept of digital topology. Connected components are basic information units in an image. Digital topology has straightforward application to binary images where regions,

edges, and object boundaries can be defined and located with precision. Rosenfeld [8] extended digital topology from binary to multivalued images by modeling an intensity image as a fuzzy set. If the intensity values are scaled in the range $[0,1]$, the gray level of a pixel can be associated with its degree of membership in the set of high-valued or “bright” pixels.

2.1. Fuzzy Topology

Let Σ be a rectangular array of integer-coordinate points. A pixel p at coordinates (x, y) is a member of Σ . Then a fuzzy subset W of Σ is a set of ordered pairs, $W = (p, \mu_W(p))$ for all $p \in \Sigma$, $\mu_W(p)$ is a membership characteristic function which indicates the degree of membership (DOM).

Let W be a fuzzy subset of Σ and let $\sigma : p = p_0, p_1, p_2, \dots, p_n = q$ be any path between two points of W . The strength $S_W(\sigma)$ of σ is defined as the strength of its weakest link

$$S_W(\sigma) \equiv \min_{0 \leq i \leq n} \mu_W(p_i) \quad \forall p_i \in \sigma \quad (1)$$

Fuzzy topology defines the concept of degree of connectedness which is the quantification of spatial ambiguity in multilevel images. Every ordered pair (p, q) of pixels are coupled by a real number in interval $[0,1]$. This value is the degree of connectedness (DOC) of p and q . In practice, pixel values are not scaled. By definition, the degree of connectedness between two points p and q is defined as the strength of the strongest path of all possible paths connecting p and q [36].

$$C_W(p, q) \equiv \max_{\sigma} S_W(\sigma) \quad \forall \sigma : p, \dots, q \quad (2)$$

Two points are p and q connected in W , if $C_W(p, q) = \min(\mu_W(p), \mu_W(q))$. Senel [9] introduced the concept of degree of connectedness map to depict how a pixel, $o \in W$ is connected to the others. Degree of connectedness map (DOCM) is defined as

$$DOCM_W(o) = C_W(o, p) \quad \forall p \in W \quad (3)$$

DOC maps can be used to remove image components that are not connected to the center pixel. In doing so, a new observation window is obtained by replacing pixel values with their degree of connectedness values to the center. Despite the vague expression “all possible paths connecting two points”, DOCM can be computed algorithmically [9]. DOCM has some interesting properties that make it the fundamental concept for the method proposed in this paper.

2.2. Degree of Connectedness Map

For clarity, properties of DOCM are explained on one dimensional drawing. Although two dimensional scenes may behave in a different way due to multiple paths exist between any two pixels, we believe that examples in one dimension would be clear enough to understand what DOCM operation does.

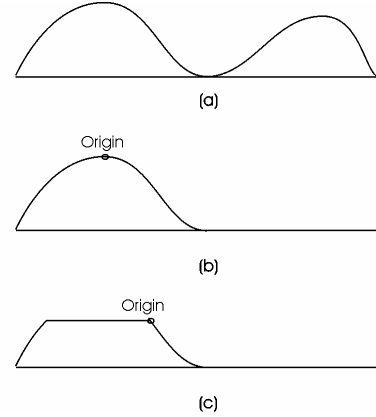


Fig. 1. a) One dimensional cross section of two close objects, b) Degree of connectedness map (DOCM) with respect to the origin, c) DOCM with respect to another origin.

Fig. 1.a. shows a cross section of an image with two parallel lines. If the degree of connectedness map is constructed with respect to the origin (Fig. 1.b.), the object on the right is not seen in DOCM. Therefore, DOCM representation has objects that are connected to the origin. If the origin is not located at the intensity maxima of the object (Fig. 1.c.), the object on the left is truncated. Therefore, DOCM removes components unconnected to the origin as well as some part of the object depending on the intensity value of the origin. Such a behavior may seem undesired at first glance since it affects gradient magnitude along the edge. Unconnected objects are removed at the expense of deformation. Reader may refer to [11] for other properties of DOCM.

3. TOPOLOGY BASED GRADIENT OPERATORS

A method must be devised so that larger kernels are used but does not allow unconnected close image components to affect the edge detector output. All data lead us to use DOCM on larger windows and calculate derivative, or gradient with kernels larger than 5×5 .

Let I be an image with pixels $p(x, y)$, and $I(x, y)$ is the intensity value of the $p(x, y)$. Let W be an $(2n+1) \times (2n+1)$ observation window. DOCM for bright pixels at the coordinates (x, y) on I is computed as

$$DOCMb(x, y; x_0, y_0) = \begin{cases} C_w(p(x, y), p(x_0, y_0)) & x_0 \in [x-n, x+n], \\ & y_0 \in [y-n, y+n] \\ 0 & \text{elsewhere} \end{cases} \quad (4)$$

Similarly but for dark pixels, DOCM for dark objects $DOCMd$ is calculated on the negative image.

Let g_x and g_y are gradient operators with a kernel size of $(2k+1) \times (2k+1)$ elements. In practice, DOCM window must be larger than the size of the kernel. Topological gradients along the x axis for dark and bright objects are

$$TG_x^b(x, y) = \sum_{\forall x_1, y_1} DOCMb(x, y; x_1, y_1) g_x(x_1, y_1) \quad (5)$$

where $x_1 \in [x-k, x+k]$, $y_1 \in [y-k, y+k]$ and g_x is the operator for the x axis. $TG_x^d(x, y)$ is calculated similarly using $DOCMd$.

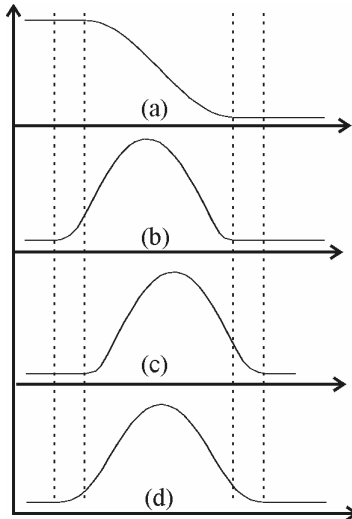


Fig. 2. a) slowly varying edge, b) $DOCMb$ with Sobel kernel, c) $DOCMd$ with Sobel operator, d) Edge boundaries of conventional Sobel gradient

For conventional operators, such as Sobel, gradient becomes significant on the region where the intensity change occurs as well as some of area around the edge (Fig. 2d). For larger kernels, the gradient becomes significantly thicker. However, due to the asymmetric behavior of $DOCMb$, gradient is biased to the bright side for slowly varying edges (Fig. 2b). Similarly, gradient is biased to the dark side with $DOCMd$ (Fig. 2c).

Therefore, it seems that information obtained from $DOCMb$ and $DOCMd$ based gradient calculations supplement each other. If the minimum value of $DOCMb$ (Fig 2b) and $DOCMd$ (Fig. 2c) based gradient values is taken as the gradient operator output, the gradient magnitude becomes nonzero in the area where the intensity

changes occurs (Fig. 3b). The topological gradient is then defined as

$$TG = \min(TG^b, TG^d) \quad (6)$$

TG tolerates the use of larger kernels since gradient residue around the edge due to large kernel size does not occur. This result is the main contribution of this paper.

4. RESULTS

In this section, the performance of TG with Sobel kernel is investigated. Results obtained with conventional Sobel are compared to that of TG with Sobel. Here, our intension is to demonstrate how to integrate DOCM representation into any gradient calculation. We believe that if integration of DOCM with any gradient operator is shown to perform better than the conventional one, any gradient operator coupled with DOCM should also yield better results.

A synthetic 1000x90 pixel image with a ramp edge is formed. One row of the image is calculated as follows

$$I(p(l)) = \begin{cases} 200 & l \leq 43 \\ 200 - 5(l - 43) & 44 \leq l \leq 62 \\ 100 & 63 \leq l \leq 90 \end{cases} \quad (7)$$

Different levels of Gaussian noise are added into the image and a series of noisy images are generated. Then, $(2k+1) \times (2k+1)$ Sobel operator and $(2k+1) \times (2k+1)$ Sobel inside $(2k+3) \times (2k+3)$ DOCM are applied on images contaminated with additive Gaussian noise of variances 5, 10, 15 and 20. The size of DOCM should be slightly larger than the kernel of the gradient operator. If very large sizes are used, two points may get connected over a path that is outside the span of the gradient kernel. Using slightly larger DOCM than the gradient kernel ensures the locality of the solution.

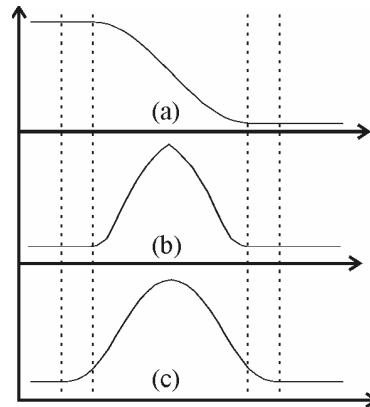


Fig. 3 a) slowly varying edge, b) proposed topological gradient, c) boundaries of conventional gradient

In order to observe how both methods react to noise, two features need to be examined. First, we need to measure how much the gradient spreads over the edge due to kernel

size. For objectivity reasons, this value needs to be compared to the magnitude calculated on the edge. This way, the amount of spread across the edge can be measured. We define the magnitude blur rate (BR) for any image row as

$$BR = \frac{\sum_{l=e_1-k}^{e_1-1} G(p(l)) + \sum_{l=e_2+1}^{e_2+k} G(p(l))}{\sum_{l=e_1}^{e_2} G(p(l))} \quad (8)$$

where e_1 and e_2 are the pixel locations that marks the beginning and the end of the edge, and k is the half size of a $(2k+1) \times (2k+1)$ gradient kernel.



Fig. 4 a) Topological Sobel 9x9 on a 11x11 DOCM b) Conventional Sobel 9x9

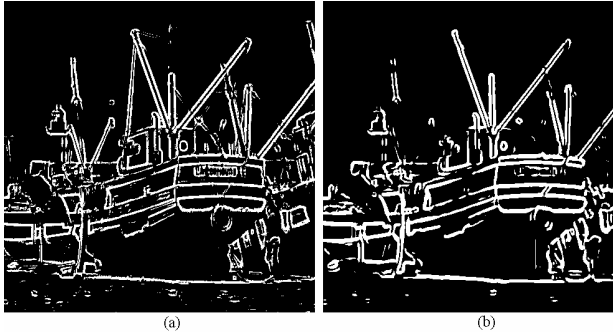


Fig. 5 a) Topological Sobel 9x9 on a 11x11 DOCM (threshold at the level 2.5 x image mean), b) Conventional Sobel 9x9 (threshold at the level 2.5 x image mean)

The second feature is to measure the resilience of the method against noise. Standard deviation of magnitudes on the flat area can be used as a measure. Resilience against noise, R , is defined as

$$R^2 = \frac{\sum_{l=1}^{e_1-k-1} (G(p(l)) - m_g)^2}{e_1 - k - 2} \quad (9)$$

where m_g is the sample mean of the flat area. Table I shows the magnitude blur rates for different noise levels.

We validate the efficacy of the topological filters using Lena image. Lena image has some challenging features for edge operators. For instance, feathers on the hat, shadows on the face, blurry background and eyes are difficult to handle. Fig 4.a is the result of topological Sobel. Fig. 4.b is calculated by conventional Sobel. It is seen that topological Sobel output has thinner lines than the other. On the other hand, Fig. 5.a and 5.b shows the results of topological and conventional Sobel operators applied on the “boat” image, respectively. The topological operator is seen to pick up more details than the conventional one.

TABLE I
BLUR RATES FOR DIFFERENT NOISE LEVELS

Noise σ	11x11 Sobel in 13x13 DOCM	11x11 Sobel		
	BR	R	BR	R
0	0.000	0.00	0.099	0.00
5	0.164	19.31	0.176	47.16
10	0.203	38.88	0.216	95.55
15	0.235	57.65	0.251	142.98

5. FUTURE WORK

The idea of integrating DOCM into the gradient calculation is the main contribution of this paper. It is also shown that for slowly varying edges, topological gradient is better than the conventional filter. Integration of DOCM into other edge detection methods needs to be investigated.

6. REFERENCES

- [1] Marr D. and Hildreth E., “Theory of edge detection,” Proc. R. Soc. Lond. A, Math. Phys. Sci., vol. B 207, pp. 187–217, 1980.
- [2] Canny, J.F., “A computational approach to edge detection”, IEEE Transactions on Pattern Analysis and Machine Intelligence 8 (6), 1986, pp. 679-698.
- [3] van der Heijden, F., ‘Edge and Line Feature Extraction Based on Covariance Models’, IEEE Transactions on Pattern Analysis and Machine Intelligence, Vol.17, No. 1, Jan. 1995.
- [4] Konishi S., et al. “Statistical Edge Detection: Learning and Evaluating Edge Cues”, , IEEE Transactions On Pattern Analysis And Machine Intelligence, Vol. 25, No. 1, pp. 27-74, 2003.
- [5] Suzuki et al, “Neural Edge Enhancer for Supervised Edge Enhancement from Noisy Images”, IEEE Transactions On Pattern Analysis And Machine Intelligence, Vol. 25, No. 12, 2003.
- [6] Fleck, M, “Multiple Widths Yield Reliable Finite Differences”, IEEE Transactions on Pattern Analysis and Machine Intelligence, Vol. 14, No. 4, 1992.
- [7] Azaria et al, “The Design of two dimensional Gradient Estimators Based on One-Dimensional Operators”, Trans. On Image Processing, Vol. 5, No. 1, 1996.
- [8] Rosenfeld, A., “fuzzy digital topology,” Information and Control, vol. 40, no. 1, pp. 76-87, Jan. 1979.
- [9] Senel H.G., et al “Topological Median Filters”, IEEE Transactions On Image Processing, Vol. 11, No. 2, 2002.